[SSC21-XIII-05]

Observing and Tracking the Great Pacific Garbage Patch

Chris Greenly, Hannah Gray, Hueson Wong, Samuel Chinn, James Passmore, Prisilla Johnson and Yaseen Zaidi
The University of the West of England
UWE Bristol, Frenchay Campus, Coldharbour Ln, Bristol, BS16 1QY, United Kingdom
chrisgreenly@hotmail.co.uk

ABSTRACT

The subtropical waters between Hawaii and California are currently infested with an accumulation of plastic estimated to be twice the area of Texas, otherwise known as the Great Pacific Garbage Patch (GPGP). This paper presents a novel CubeSat mission to monitor the size, growth and position of the GPGP. At 1.6 million square kilometres, the GPGP is by far the largest and most serious accumulation of garbage out of the five patches littered across the world's oceans. If we are to prevent further damage to the marine ecosystems, it is imperative we act with the utmost urgency. Leveraging recent technological advancements in imaging capabilities, a comprehensive concept of operations has been produced detailing the satellite's lifecycle from launch to deorbit, including the crucial phases whereby data is collected and transmitted. Although this paper focuses on tracking and monitoring the GPGP, the same concept of operations has the potential to observe all five garbage patches. The proposed mission utilises two reflective indices, Normalised Difference Vegetation Index (NDVI) and Floating Debris Index (FDI), that will aid in differentiating surface plastics from other floating materials. For the mission to employ both NDVI and FDI, the chosen payload will require a spectral capture range from 665nm (red edge) to 1600nm (Short Wave Infrared) and would ideally have a Ground Sampling Distance (GSD) of no greater than 10m to guarantee the data collected is valuable.

INTRODUCTION

In the North Pacific Ocean, there is an estimated 80,000 tonnes of floating garbage, collectively known as the Great Pacific Garbage Patch (GPGP)[1]. Across the globe, there are five ocean garbage patches of which the GPGP is the largest.

The presence of garbage in the ocean is detrimental to marine ecosystems and may ultimately have negative health and economic implications for humans if not dealt with. Around 52% of the mass of the GPGP is from fishing nets[2] which can entangle marine life as shown in Figure 1, and smaller plastics often get confused for food, resulting in malnutrition[1].

Figure 1: Sea Turtle Entangled in Discarded Fishing Net[3]

Another problem is that 84% of ocean plastics have one or more Persistent Bio-accumulative Toxic (PBT) chemicals in their composition[4] which, if consumed by marine life, eventually travels up the food chain, ultimately resulting in PBT chemicals being consumed by humans.

Ocean plastics cause an eyesore to natural beauty spots. To combat this, governments or local councils must attempt to remove the garbage. With mounting pressure from tourists, fisheries and aquaculture industries, they have been forced to exhaust time and money removing the waste[1]. Therefore, reducing the impact of ocean garbage has become an increasingly discussed topic due to the damaging impact it is having on the planet, socially, economically, and environmentally.

There have been numerous expeditions to the GPGP remote it is, large small aircraft have been required to capture data[2]. While usually not stated, the cost of logistics, wages, fuel, equipment and the vehicles themselves make expeditions an expensive endeavour. Garbage samples have been collected by trawling vessels that use traps or nets and large areas of surface debris have been imaged using aircraft. These expeditions are subject to constraints such as funding, range, supplies, and weather conditions which limit the extent of area covered, and the duration and frequency of the expedition. Thus, not only is acquiring data

expensive, but the data itself may not always capture the whole GPGP. Satellite missions to observe the GPGP do not currently exist and there has been much discussion surrounding the readiness of imaging technology to capture sufficient data from space[1]. However, through various studies[5,6,7] plastics and fishing nets have been observed using satellite imagery. These studies verify that large collections of plastics in the ocean can indeed be observed and measured. The biggest drawback is the huge cost associated with satellite missions, with the Sentinel satellites costing the European taxpayer €350M[8].

This paper proposes the use of a standard low-cost satellite, known as a CubeSat, as a means to observe the growth and movement of the GPGP. The data collected by the CubeSat mission will be used to refine estimates on the size, boundary and quantity of garbage in the GPGP and complement those studies already conducted by trawlers and aircraft. The mission aim is to provide detailed, accurate data to those organisations that are attempting clean-up efforts. This will optimise their productivity and resources, which will have a positive impact on the planet.

OCEANIC PLASTIC POLLUTION

Introducing a mission to track and observe large patches of plastic in the Earth's oceans requires a level of understanding of how and why they were formed. The science behind their formation is well understood but their composition and the scale of the problem is presently just a statistical estimate. What is clear, is that drastic human intervention is now required to save the marine ecosystem from destruction.

Where is it?

Garbage patches form within the Earth's oceans due to the presence of gyres. A gyre is a circular current system brought about by the Earth's rotation and wind patterns[9]. Gyres form due to currents within the Earth's oceans caused by Ekman transport: differences in temperature and salinity which causes thermohaline circulation (Figure 2) and the Coriolis Effect. When the warmer surface currents reach the colder polar regions the water freezes forming sea ice which increases the salinity of the surrounding water; these colder, denser waters then sink to the ocean floor. The cold-water currents warm up as they approach the equator completing the system.

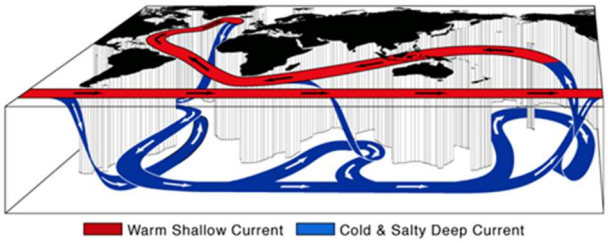

Figure 2: Thermohaline Circulation Diagram from Quibb[10]

There are five main gyres where plastic waste has been seen to accumulate: the North Pacific, South Pacific, North Atlantic, South Atlantic and Indian Ocean subtropical gyres[11]. At the centre of the gyres is a large stationary area of water where the waste within the currents accumulates and comes to rest. This leads to the formation of garbage patches; the most famous and largest of which is the GPGP which is found in the North Pacific Subtropical gyre. In the Indian Ocean subtropical gyre, the plastic waste is more sparsely distributed than the other four due to the interaction of the Agulhas current between Madagascar, Mozambique and the currents from the southwest Pacific Ocean[11]. The interaction of the Agulhas current leads to larger concentrations of plastic pollution being found closer to the South African and Madagascar coastlines[12]. The Indian Ocean gyre is also affected by the Monsoon season, which disturbs the wind direction causing changes in surface currents via Ekman transport, which then causes plastic waste to be deposited on the coastlines[13]. The oceanic regions around the equator and the Antarctic Ocean generally have lower levels of plastic pollution due to the high levels of Ekman transport[11].

Whilst gyres have high accumulations of plastic pollution, a study by Chenillat *et al.*[11] found that between 54% and 70% of plastic waste gets deposited on the coastlines instead of the open water ocean gyres. This estimate, however, may be lower in the real world as the model is based on an ideal case that uses a simplified beaching process and does not consider the ocean dynamics on the coastline such as the tides. Another location of plastic pollution is the ocean floor, where plastic has either sunk due to having a higher density than the seawater or has been carried down by the thermohaline currents that supply oxygen and nutrients to the deep-sea wildlife. Kane *et al.*[14] discussed that high levels of plastic pollution could be found on the seabed. Samples collected in the Tyrrhenian Sea had approximately 1.9 million microplastic pieces per square meter. Their findings show that the plastic pollution visible on the surface may just be a fraction of the pollution in the Earth's oceans. The problem of how the plastic travels around the oceans and where it ends up is

still largely unknown[15]. This is because most of the studies and models of plastic pollution and its mechanics are based on a small number of sampling expeditions, opening the door for a larger and wider spread method of researching the movement of plastic pollution within Earth's oceans[16].

It is worth acknowledging that as the climate changes, so will the dynamics present within the ocean; with seawater changing temperature, salinity and current patterns - more plastic may end up sinking to the seafloor. Along with these dynamics, the increasing frequency of extreme weather patterns could also lead to a change in how plastic pollution collects within our oceans, with a potential increase in coastline deposits[17]. These extreme weather patterns could also increase the amount of pollution entering Earth's oceans as seen with the Great Japan Tsunami of 2011[18].

How does it get into the oceans?

It is estimated that 80% of oceanic plastic pollution originates from land-based sources with 20% originating from marine sources[19]. Examples of marine sources are discarded fishing nets, lines, ropes and rarely, abandoned vessels. Land-based sources cover plastic waste that finds itself in the oceans after either being littered or originating from mismanaged plastic waste. Littered waste is waste that is not disposed of through official methods. Whereas mismanaged plastic waste is plastics that enter the oceans either through landfill run-off, uncontrolled disposal of plastics as well as poor waste management and recycling practices[17,20]. Using the data collected by Jambeck *et al*.,[19] Ritchie and Roser[21] showed that in 2010 the largest region responsible for plastic pollution entering the oceans is East Asia and the Pacific region, with 60.1% of waste originating from that region. A breakdown of the amount of plastic waste mismanaged by each country can be seen in Figure 3. Whilst it can be seen that Indonesia, India and China have higher levels of mismanaged plastic waste, they also import plastic waste from countries such as Germany and the United Kingdom. The transport of plastic recycling to these countries has a large potential for waste leakage into the oceans before it arrives to be processed in East Asia. Bishop, Styles and Lens[20] acknowledged that a higher level of plastic mismanagement is seen in these countries as they have lower quality waste processing systems than those seen in wealthier nations in the West; this correlates with the findings of Jambeck *et al.*[19].

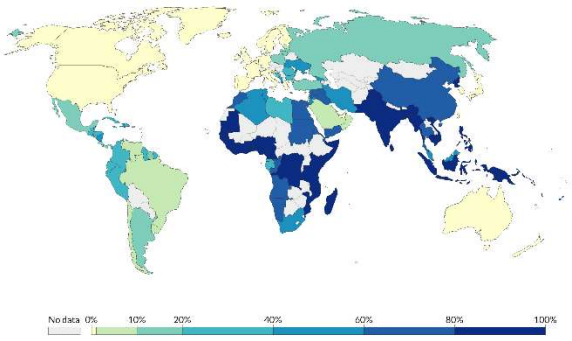

Figure 3: Mass of Plastic Waste from Mismanaged Disposal in 2010, Presented by Ritchie and Roser[21] using Data from Jambeck *et al.*[19].

In 2018, Polyethylene accounted for 30% of European plastic. Bishop, Styles and Lens[20] estimate that from the European Union (EU) in 2017, the United Kingdom and Germany contributed the highest levels of ocean debris from polyethylene export recycling, at 29% and 32% respectively. Figure 4 shows that mismanaged plastic waste is just part of the problem. Large amounts of plastic waste being littered has a high chance of entering rivers and oceans, ultimately increasing pollution levels.

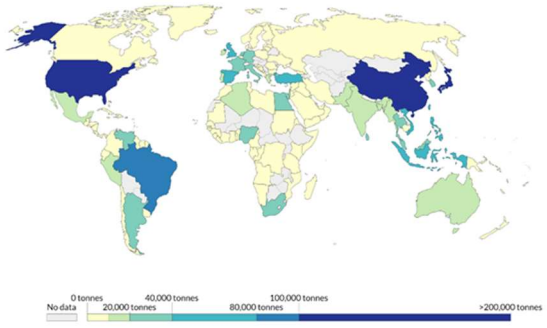

Figure 4: Mass of Plastic Waste Littered in 2010, Presented by Ritchie and Roser[21] using Data from Jambeck *et al.*[19].

The findings of Lebreton *et al.*[22] align with those of Jambeck *et al.*[19] who found that Asia was responsible for 86% of global river plastic pollution in 2015; with 6 of the 20 most polluting rivers found flowing through China. The Yangtze river alone has an annual input of 333,000 metric tonnes followed by the River Ganges at 115,000 metric tonnes of plastic waste which eventually finds its way into the ocean.

It is estimated that lost fishing equipment makes up 10% of all ocean plastics from marine sources. However, due to their higher mass, compared to microplastics, lost fishing equipment accounts for a larger percentage of the total mass of plastic debris in the oceans[21]. On a smaller scale, plastic waste can also enter the oceans from trade.

It is uncommon for shipping containers to be lost to the ocean, with an average annual loss of only 779 containers over the period of 2017-2019[23,24]. Turner, Williams and Pitchford[23] cite the findings of Galafassi, Nizzetto and Volta[25] that around 10,500 metric tonnes of plastic enter the oceans annually from lost cargo. Lost cargo can be hard to track and document as it does not need to be reported unless the cargo provides a hazard. This could imply that the current estimates of lost cargo are less than the true amount[23]. Whilst plastic pollution from lost cargo contributes to less plastic pollution than other sources; when a shipwreck occurs, thousands of containers can be lost to the ocean, causing a large amount of plastic waste to enter the oceans. This was seen in 2013 when the MOL Comfort sank off the coast of Yemen losing 4,293 of its 4,382 cargo containers[24,26].

The Great Pacific Garbage Patch

The most renowned collection of plastic pollution is the Great Pacific Garbage Patch that is found in the North Pacific gyre. It is estimated to have a total mass of 96,400 metric tonnes, made up of 1990 billion pieces[21,27]. Plastics account for 99.9% of the debris within the GPGP[2] of which 94% of the debris pieces are microplastics. However, these microplastics only make up 8% of the total mass of the patch. The larger plastics (macroplastics and megaplastics) have been shown to represent more than 75 % of the total GPGP mass. These larger plastics are made up of mostly rigid Polyethylene (PE) and Polypropylene (PP) plastics, and discarded fishing nets remaining afloat[2]; with fishing gear consisting of 52% of the total mass[21]. At least half of the plastic debris is expected to float as it is less dense than seawater with High-Density Polyethylene (HDPE) having a density of < 970 kg/m^3 [11,16]. It is worth noting, that as more freshwater enters Earth's oceans from polar ice melt the salinity of water will decrease causing greater amounts of plastic pollution to sink[17].

Stevens[15] estimates the mass of the GPGP at 80,000 metric tonnes, which is lower than the estimate already discussed. These discrepancies, along with the estimated total annual input of plastic waste being greater than the estimated amount of pollution in the oceans (268,940 metric tonnes[27]) arise from the uncertainty of how much plastic is actually within the oceans. This could be due to several factors. For example, there is still a large uncertainty with how much plastic waste is present on the seafloor,[14,15] along with vastly overestimating the amount of plastic pollution that enters the ocean, or underestimating the amount floating on the surface of the ocean. Other explanations are that the missing plastics have been ingested by organisms or buried within the coastlines[21]. This uncertainty of the amount and the movement of plastics within the Earth's oceans requires more methods to fully understand the full picture of the problem and to allow for solutions to be better targeted to clean up the plastic pollution.

OBSERVATION METHODS

Since the majority of debris in the GPGP is plastic, observation methods typically involve identification either visually or through spectral analysis. The possible methods are described in the following sections.

Infrared Imaging

Maximenko *et al.*[28] present various examples of different types of sensors that are currently being used to detect plastic debris. The sensor bands are either multispectral or hyperspectral, capturing wavelengths from the ultraviolet to the Far Infrared (FIR) range. Garaba and Dierssen[29] found the presence of unique spectral absorption features in the Near Infrared (NIR) and Short-Wave Infrared (SWIR) spectrum through experiments on microplastics washed ashore the United States from the Pacific. These absorption features were insensitive to the size of the plastics observed. Similarly, when comparing wet samples to dry samples, although the magnitude of reflectance somewhat decreased, the spectral reflectance shape of the samples was retained allowing them to be detected. The results of the study undertaken by Garaba and Dierssen[29] suggest that floating microplastics can be successfully detected using detectors capturing light in the NIR or SWIR spectrum. That being said, water absorbs light in the NIR range and this study did not investigate the reflectance of the samples partially or fully submerged.

NIR spectroscopy (NIRS) is a technique that uses spectra in the NIR region of the electromagnetic spectrum (780 nm – 2500 nm)[30]. Zhu *et al.*[31] present a successful method for identifying plastic waste using NIRS capturing wavelengths in the range of 900 nm – 1700 nm. The method investigated involved recording each of the spectra related to the following plastic groups: PE, PP, Polymethyl Methacrylate (PMMA), Polyethylene Terephthalate (PET) and Acrylonitrile Butadiene Styrene (ABS). The spectral acquisition time was roughly 0.5 second. Due to the relatively long spectral acquisition time, the detection platform used contained a very small number of pixels, thus yielding a low-resolution image. Nonetheless, each of the plastics used in the experiment were successfully detected with all but three of PE's spectra being correctly identified as seen in Table 1.

Table 1: Identification Result of NIRS Technique[31]

Plastic group	Number of spectra	The number of correctly identified spectra
PS	20	20
PP	20	20
PMMA	20	20
PET	20	20
PE	20	17
ABS	20	20

Following investigation, pre-processing was found to greatly improve the identification of each of the plastics and using a principal component analysis (a method used to reduce the dimensionality of a data set) allowed each of the six plastic types to be identified.

Microplastics measuring less than 4.75 mm have been found to represent just 13% of the buoyant debris making up the GPGP[2]. Some degree of the remaining buoyant plastics may be partially submerged[32] and therefore difficult to capture via NIR or SWIR spectroscopy. On the other hand, NIR or SWIR spectroscopy has been proven to be an effective means of detecting unsubmerged (floating) plastics, as the IR-absorbing sea creates a dark background. As part of the Ocean Cleanup initiative, a C-130 aircraft flew over the Pacific Ocean and began detecting floating plastic debris using an onboard SWIR imager, which was proven successful in detecting objects greater than 0.5 m in size[1].

Detecting the spectra reflected by plastics when partially submerged underneath water, is of great importance of observing the GPGP in its entirety. High-spatial-resolution observation methods by satellites using light within the visible spectrum (400 – 700 nm) has been successfully used to observe and track marine debris comprised of floating and slightly submerged objects. Readily available commercial high-spatial resolution imagers are usually limited to a resolution of 25 – 50 cm, making them only useful for identifying objects of several meters[28]. In a recent study by Biermann, L. *et al.*[33] using data from the European Space Agency (ESA) Sentinel-2 satellites, NIR spectroscopy has further proved successful in observing floating plastics in the open ocean. It was found that pixels comprised of at least 30% plastic bottles or bags, or 50% plastic fishing nets allowed the reflected wavelengths characteristic of plastics to be observed. The study found in addition, that seaweed absorbs wavelengths within the SWIR region at 1610 nm which, like the ocean's absorption characteristics, should make observing floating plastics easier. Similarly, pumice – a volcanic rock material that often forms natural rafts in the ocean, was found to absorb light in the NIR region at around 830 nm.

Potential methods for observing fully submerged plastic debris have been suggested, such as Raman spectroscopy: a type of vibrational spectroscopy which works by exciting a target using a laser source and subsequently observing the peaks related to the target's vibrational modes[34]. Raman spectroscopy has been successfully used for observation activities in the deep ocean. However, the method operates using a low power laser, giving weak signals which can be drowned out by excessive noise, and with current technology are difficult to detect using satellites[28].

Spectrometers capturing wavelengths between the NIR and SWIR electromagnetic spectrum present potential means for detecting floating surface plastics in the GPGP. High-spatial-resolution sensors capturing wavelengths in the visible light spectrum may struggle to distinguish floating plastics from the background seawater or other floating material, such as pumice or vegetation. No experiments have been found presenting data for observation of submerged plastics; therefore, it may be difficult to observe the GPGP in its entirety (including the less buoyant plastics) from space. Due to the scale of the GPGP, observations of only surface plastics are likely to yield a reasonable accuracy of the size and position of the GPGP relative to its size.

Reflective Indices

The plastic debris within the GPGP may also be in close proximity with a variety of other materials and therefore it would be beneficial to recognise and distinguish plastics from vegetation, pumice or any other natural occurring floating material. Investigating past and current methods which use satellites to identify vegetation from space could provide insight into a method that could be applicable for the proposed mission.

One of the primary techniques in this area is the use of the Normalised Difference Vegetation Index (NDVI) to identify and measure vegetation. In simple terms, NDVI is a measure of the health of vegetation, based on how plants reflect certain wavelengths within the electromagnetic spectrum[35]. A plant varies in its NIR absorption rate dependent on the composition of the chlorophyll in the plant pigments. More chlorophyll will absorb a greater amount of red light and reflect NIR. Satellite sensors use this information to measure the different wavelengths of light absorption and reflection by plants. Plotting this data forms a stoplight colour map. This method is used largely by scientists in agriculture fields to monitor vegetation around the world, especially in areas with high chances of drought, for precision farming, measuring biomass and to compute forest supply and leaf area index[36]. Sentinel-2, Landsat and SPOT missions have been instrumental in producing red and NIR images. The equation to calculate the NDVI is shown in Equation 1.

$$NDVI = \frac{R_{rs,NIR} - R_{rs,RED}}{R_{rs,NIR} + R_{rs,RED}} \quad (1)$$

Where R is the reflectance value, and the subscripts NIR and RED follow the notation used by Biermann *et al.*[33].

The NDVI is calculated for every datapoint and is usually between the range of -1 and +1. A high NDVI value indicates the NIR reflectance reading is greater than the RED channel, meaning that there is healthy vegetation at that location. A low value indicates either less or no vegetation[37]. As can be seen in Figure 5, different materials can be clearly distinguished based on the value they produce using NDVI.

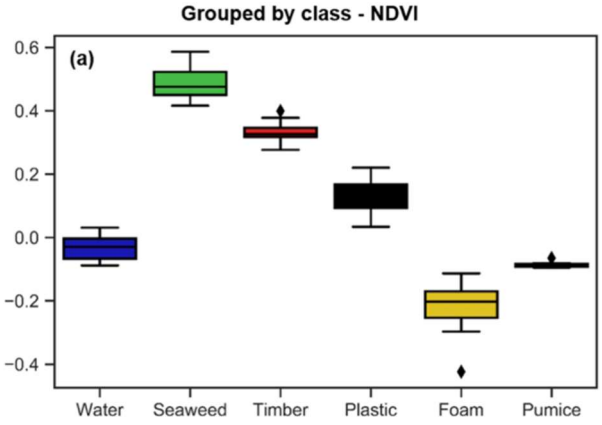

Figure 5: NDVI Values for Different Materials[33].

Though the proposed mission is not specifically looking at vegetation health, NDVI could aid in distinguishing vegetation found in the ocean from floating plastics. Similarly, to detect aggregations of floating debris at subpixel scales, a Floating Debris Index (FDI) has been developed by Biermann *et al.*[33] for the Sentinel-2 Multi-Spectral Instrument (MSI). Where NDVI is useful for distinguishing types of debris, the quantity of debris within a pixel determines the FDI value. The FDI by Biermann *et al.*[33] is given by Equation 2:

$$FDI = R_{rs,NIR} - R'_{rs,NIR} \quad (2)$$

$$R'_{rs,NIR} = R'_{rs,RE2} + \left(R_{rs,SWI} - R_{rs,RE2}\right) \times \frac{(\lambda_{NIR} - \lambda_{RED})}{(\lambda_{SWI} - \lambda_{RED})} \times 10 \quad (3)$$

Imaging Methodology

The satellite imaging device must be considered against several factors to identify its suitability for a mission. For example, there are different ways for a camera to scan an area: framing, whisk-broom scanning, and push-broom scanning. While the satellite travels along its orbit, a push-broom scanning technique allows images to be taken in the along-track direction which provides a larger ground area to be observed. This method is ideal for capturing the GPGP since it covers a vast area.

Arguably the most critical factor when choosing a suitable payload is the spectral range available. Previous studies suggest that a spectral range spanning at least from the red edge of the visible spectrum to the NIR region should allow floating plastics to not only be observed, but to be distinguished from other natural floating material through the use of the NDVI.

Another key factor that must be considered when identifying a suitable payload is the imager's Ground Sample Distance (GSD) – the distance between the centre of two adjacent pixels as measured on the ground. Based on the current understanding of the GPGP, items of floating plastic debris can range in size from several meters such as discarded fishing nets, down to a few centimetres. To produce successful results comparable to the findings of Biermann *et al.*[33] the imager's GSD should not exceed 10m. A smaller GSD may be desirable to observe finer details but will consequently result in larger amounts of data being collected. The resolution of the imager and the satellite's altitude will jointly impact the GSD achievable.

Similarly, the temporal resolution of the imager - the time between flyovers over an area of interest must be considered – which can be directly adjusted depending on mission parameters. For features that change rapidly, a higher temporal resolution may be desired to track small changes. Radiometric resolution - the capacity of the imager to distinguish differences in light intensity or reflectance will also have to be studied and confirmed as suitable. The greater the radiometric resolution, the more detailed the sensed image will be[38]. These factors are all ways of determining the capability and suitability of the payload against the mission requirements.

MISSION IDENTIFICATION

Plastics have emerged as a readily accessible and cheap material but have issues with biodegradability, disposability and after-life. Many products end up in landfills and water bodies like the Earth's oceans, which endanger ocean ecosystems and organisms. Government bodies need an effective system that can give a holistic image of the largest assemblage of ocean plastics – the Great Pacific Garbage Patch and eventually, technology needs to be demonstrated that can capture data about growth rate, size, composition, point of origin and movement of not only the GPGP but all the Earth's garbage patches.

To date, gathering information on the GPGP has relied on trawler expeditions and aircraft flyovers. Which although have proven vital in the understanding of the

GPGP, have also brought a great deal of uncertainties in the data. As such, the current picture of the GPGP is comprised of a series of statistical approximations. Due to the vast scale of ocean garbage patches, a satellite observation mission by means of an affordable CubeSat offers an ideal solution to the problem.

CONCEPT OF OPERATION

The concept of operation, which describes the lifecycle of a CubeSat and how it will operate, from launch through to decommission and disposal is described next.

Mission Overview

The mission has been split down into several phases, which describe the different operations of the mission, as shown in Table 2.

Table 2: Con-Ops Mission Phases

Mission Phase	Operation
Launch	Via a rocket with multiple payloads
CubeSat Deployment	Poly Picosat Orbital Deployer (P-POD) or another suitable dispenser will be used for ejection into orbit
Wait/Sleep	To avoid communication interference with other deployed satellites and save power
Acquire Orbit	Achieve desired altitude and inclination
Detumble	Reduce angular rates and stabilise orientation for imaging and communication
Release Solar Panels and Antennas	Use spring, burn wire or any suitable mechanism to release
Communicate with Ground Station	Establish a link with mission base, relay health stats and ensure the hardware is operational, calibrate on-board sensors
Observe Garbage Patch and Communicate with Ground Station	Begin primary mission of observation and relaying data
Orbit Decay	Decay after ~2.5 years
Disposal	Dispose of CubeSat safely

A low earth, Sun-Synchronous Orbit (SSO) has been chosen which will allow the satellite to pass over any given point at the same local time. Additionally, an SSO will provide consistent lighting as to adequately charge any on-board batteries using solar arrays and will provide a consistent illumination angle on the planet every time it passes overhead, particularly useful for imaging in visible or IR regions of the electromagnetic spectrum.

The CubeSat will most likely be launched from a rocket vehicle carrying multiple payloads. The exact means of launch will depend on what is available near the time of launch.

Generally, multiple CubeSats are deployed one at a time; the wait period restricts satellites from making collisions, transmissions or performing any operations until they spread out, to prevent interference.

Next, communication needs to be established between the ground station and the satellite to verify that it is on the correct orbit and allow predictions to be made regarding the trajectory. Vital statistics will be retrieved about the health of on-board hardware to ensure the mission can be initiated successfully. A 'stand-by' period will be used to validate the satellite operations in orbit with those that were conducted on the ground before launch, such as the image quality and data transmission rates.

Once all operations have been fully validated, the satellite will enter the main mission phase where it will complete many cycles of observation and data transmission. During operation, the satellite will begin to decay due to atmospheric drag in the Low Earth Orbit (LEO). Estimates suggest it may take roughly 2-3 years for the satellite to enter the Earth's atmosphere based on an altitude of 570km. For this reason, the operational lifetime of the mission is expected to last a maximum of 2.5 years, which should provide a wide enough window to gather useful data about the GPGP.

Mission Modes

The satellite will have four modes during its main mission phase: *Idle, Observation, Downlink* and *Safe*. The descriptions of these modes are outlined in Table 3.

Table 3: Mission Mode Overview

Mode	Purpose	Orientation	Components "On"	Components "Off"
Idle	Housekeeping data collection, health beacons, UHF uplinks, Re-Charging	Sun facing	- UHF Beacon - ADCS - GPS	- Camera - S-Band (Downlink)

Observation	Imaging GPGP	Earth facing	-Camera - GPS - ADCS	- S-Band - UHF Beacon
Downlink	S-Band Downlinks to transfer data to the ground station (GS)	Earth facing	- S-Band - GPS - ADCS	- Camera
Safe	Conserve Power, Re-charging	Sun facing	- UHF Beacon - ADCS - Sensors	- Camera - S-Band - GPS

Figure 6 presents a visual representation of the mission modes, showing the satellite's expected orientation and highlighting when key tasks such as imaging and downlinking may take place.

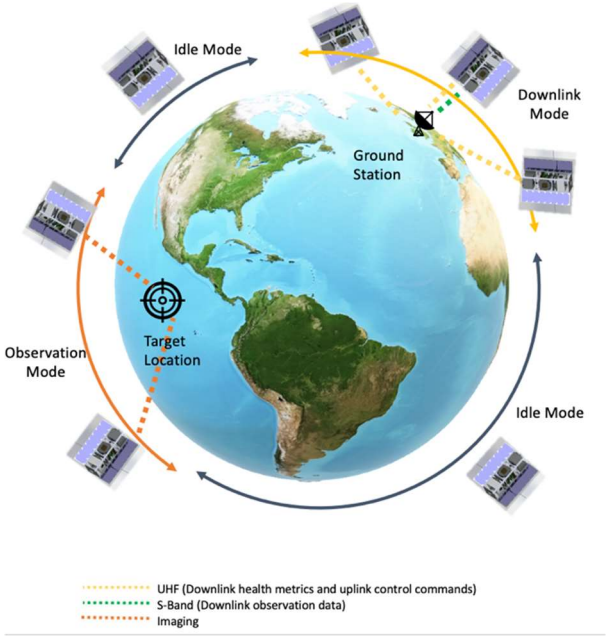

Figure 6: Visual Schematic of Main Mission Modes

Figure 7 shows a systematic block diagram that describes the requirements for each mission mode to be activated. The mission's default mode is *Idle* where the CubeSat will rest and re-charge using the solar panels, whilst collecting health metrics and receiving commands in the Ultra High Frequency (UHF) uplinks. It will then either switch to *Observation*, *Downlink* or *Safe* mode when required.

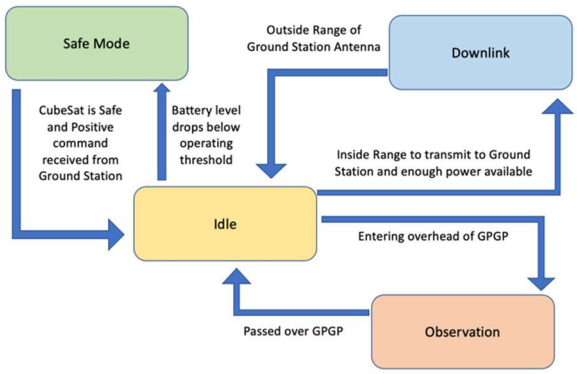

Figure 7: Systematic Representation of Mission Modes

Idle is the typical mode of the satellite. When not observing the GPGP or downlinking data, the satellite will orientate itself so that the solar panels directly face the sun using external sun sensors and an Attitude Determination and Control Subsystem (ADCS) unit. This provides optimal charging of the batteries while vital information regarding component health is collected. Un-required components are switched off while in this mode such as the camera and data transmitter.

The *Observation* mode is where the scientific data for the mission is collected, and the satellite is orientated with the payload facing the Earth (nadir). The payload is calibrated before any images of the GPGP are taken to minimise the efforts of post-processing. This calibration will be done before the satellite passes over the estimated boundary of the GPGP, capturing images of the ocean without any garbage. These images will provide data about the spectra emitted from a reliable baseline source in order to make distinguishing plastic spectra in the GPGP easier.

The satellite will be commanded to start image capture just before it reaches the specific GPS coordinates programmed for the over-estimated boundary of the GPGP. The on-board ADCS will help maintain the orientation of the camera pointed towards the target whilst the satellite continues along its trajectory. To help stabilise the CubeSat in observation mode, Earth horizon sensors and an on-board magnetometer can be used for acquiring attitude and reduce the effects of image blur.

The GPGP has an estimated area of 1.6 million km^2 [1]. Based on this information and the size of the North Pacific Ocean it is expected that the CubeSat will be in *Observation* mode for a maximum of 15 minutes while it passes overhead of the GPGP, which includes an additional 10% either side of the current estimated boundary. However, in most cases the observation time will be significantly less due to the path of the orbit.

After an observation pass of the GPGP, the data collected will then be stored ready to be downlinked.

The *Downlink* mode can be activated once the satellite is within line of sight of the ground station antenna (having a 90-degree field of view). During this time image data will be transferred to the ground station. Initial estimates suggest that current data transfer rates will not allow all the collected data to be downlinked during a single pass of the ground station. For this reason, multiple ground stations may be used, and data will be downlinked at every opportunity - this will avoid the undesirable risk of saturating the memory whereby no further imaging data can be stored. The downlink will take place while the CubeSat orientation is oriented with the transmitter in direct line of sight of the receiver, allowing the data transmissions to be sent without interference from any subsystems. Once the mission has commenced, the ground station team will have the flexibility to monitor and adjust these operations in order to optimise the observation data being collected.

Safe mode is designed to put the CubeSat into a sleep state if any hardware faults are reported. If this occurs, the faults are then transmitted to the ground station and the satellite waits while continuing to store solar energy. Possible reasons for causing the satellite to enter safe mode are as follows:

- Battery voltage drops below the safe threshold limit
- Hardware temperature exceeds the operating envelope of its Allowable Flight Temperature (AFT)
- Loss of communications with a component
- Irregular or excessive telemetry or power draw

If *Safe* mode is entered, ground operators must assess how to resolve this issue and revive the mission. If the issue can be resolved and the satellite is safe to resume operation, then communication will be sent to return the CubeSat to *Idle* mode.

Mission Risks and Limitations

No mission is completely free of risks or limitations. For the mission outlined above, there is a considerable risk since it has not been conducted before, and the payload technology is still immature and unproven in operation. Potential mission risks have been evaluated and scored based on their impact and likelihood, the most prominent of these risks and mitigation strategies are shown in Table 4.

Table 4: Mission Risks

Risk	Mitigation Strategy
Failed launch & unsuccessful deployment into orbit	Use standard form factor CubeSat configuration, and tested deployment mechanism
Solar panel or antenna deployment fails	Testing of deployment mechanism and process prior to launch and have a backup deployment mechanism
Camera systems fail to detect plastic wavelengths	Rigorous testing of camera equipment before launch, and conduct experiments based on simulated operating conditions
Bad weather conditions on Earth restrict observations of the GPGP	Ensure the mission lifetime is long enough to capture adequate data assuming poor weather conditions for up to 30% of its life
CubeSat component damage or failure	Have redundant systems where possible and conduct ground testing prior to launch
CubeSat damage caused by radiation	Conduct radiation analysis to implement necessary shielding of vital components. Use error correction codes and have memory and component redundancy where possible
CubeSat collides with space debris	Use a system to pre-empt debris collisions and manoeuvre CubeSat using ADCS to avoid them

Many of these risks can be mitigated on the ground before the satellite is launched through thorough analysis and simulated operation testing. The design should also include redundancies of critical systems and components so in the case they become damaged or fail, the mission is not compromised. The highest rated risks are ones that cannot easily be controlled or mitigated. For example, poor weather conditions on Earth could compromise the imaging quality whilst the satellite is overhead of the GPGP. If insufficient data is collected, then it may be impossible to build an accurate picture of the size and location of the GPGP resulting in failure of the mission objectives.

Data Acquisition

In the study conducted by Biermann *et al.*[33], 4 discrete spectral bands were used to identify floating debris as shown in Table 5. As discussed previously, the chosen payload should capture wavelengths within the NIR and SWIR regions of the electromagnetic spectrum to observe and detect floating PP and PE plastics in the GPGP. Capturing wavelengths similar to those presented in Table 5 including wavelengths towards the red end of the spectrum would allow pumice and vegetation to be distinguished from any floating plastics through the use of the NDVI and FDI indices.

Table 5: Spectral bands on the MSI used by Biermann *et al.*[33] (highlighted in bold)

MSI Band	Descriptor	S-2A Central Wavelength (nm)	S-2B Central Wavelength (nm)	Resolution (m)
Band 1	Coastal Aeroso	442.7	442.3	60
Band 2	Blue	492.4	492.1	10
Band 3	Green	559.8	559.0	10
Band 4	**Red**	**664.6**	**665.0**	**10**
Band 5	Red Edge 1	704.1	703.8	20
Band 6	Red Edge 2	740.5	739.1	20
Band 7	Red Edge 3	782.8	779.7	20
Band 8	**NIR**	**832.8**	**833.0**	**10**
Band 8a	Narrow NIR	864.7	864.0	20
Band 9	Water Vapour	945.1	943.2	60
Band 10	SWIR Cirrus	1373.5	1376.9	60
Band 11	**SWIR 1**	**1613.7**	**1610.4**	**20**
Band 12	SWIR 2	2202.4	2185.7	20

Evaluating the NDVI does not require a reflectance value in the SWIR range, but is required to calculate the FDI. Using the NDVI alone may be sufficient to detect and differentiate different types of floating debris, but the addition of FDI would significantly improve this. If both NDVI and FDI are to be employed, wavelengths spanning from 665 nm (red) to 1600 nm (SWIR) will need to be captured by the payload. It is suggested that the payload chosen is capable of capturing the four discrete wavelengths presented by Biermann *et al.*[33] to yield satisfactory results and provide confidence in the data.

Data Processing

After the satellite captures image data from the GPGP, the data gets stored to an On-Board Computer (OBC) before being transmitted to a ground station via an S-Band transmitter. The location of the ground station may be positioned anywhere globally, but it should contain all the required equipment to downlink and process the data.

Given that downlink time is a precious resource, one of the OBC's tasks is to determine what to send. However, the computational capabilities of the OBC are rather limited and can only handle light work. Nevertheless, it is intended for the OBC to discard images where there is no floating debris and where there is, attach the corresponding GPS coordinates and compress the image in a lossless format. How this will be achieved will depend on the on-board image analysis and compression capability.

After receiving the data at the ground station, it will be decompressed, stitched together, and updated onto a map so that changes can be tracked over time. The data will be available in pre and post-processed formats to aid researchers who may wish to process the data themselves. For post-processed data, atmospheric corrections, image enhancement techniques, NDVI and FDI will be applied in an automated process. Over the course of the mission, the aim is that a map of the GPGP will become populated with grid points where plastic has been identified and a time-lapse can be produced allowing the location, growth, and movement to be clearly visualised.

Launch Preparation

The preparations for launch begin with selecting the launch service provider, which will be selected based on cost, orbit, and suitability of the launch date. Due to their compact size, CubeSats are typically launched using a shared mission which provides a greatly reduced cost as opposed to having their own dedicated launch. Spaceflight offers rideshare missions to SSO for 3U CubeSats for $145k. SpaceX and Rocket Lab also offer rideshare missions, but costs are not readily available.

Launch providers often require evidence of coupled loads and thermal analysis to provide assurance that the CubeSat would survive the launch. Also, licensing for the communications will need to be agreed with the appropriate authorities before launch. Tests include thermal vacuum, vibration, radio emissions, power system, camera, deployment, and fit checks.

Decommissioning and Disposal

CubeSats are required to deorbit within 25 years of mission end as dictated globally Committee on the Peaceful Uses of Outer Space from the United Nations Office for Outer Space Affairs and nationally by agencies such as ESA and NASA[39,40,41,42] in order to comply with space debris mitigation guidelines. These guidelines are not always abided by. Between 2003 – 2014 one out of every five CubeSats successfully launched violated these international guidelines as discussed by Selding[40]. Lewis[41] found that between December 2010 and February 2014 40% of CubeSat

manufacturers launched a CubeSat that would violate these guidelines. These guidelines have been implemented to reduce the amount of debris found in orbit around the Earth. They aim to minimise collisions between decommissioned vehicles or collisions with active missions and endeavour to stop similar collections of garbage seen in the oceans from occurring in space.

Typically, the disposal method for CubeSats is for the orbit to decay and to then burn up upon re-entry into the atmosphere as this is preferred by the international guidelines[41]. To guarantee disposal via deorbit some CubeSats are being equipped with lightweight orbital breaks that act like a parachute[40] which could be implemented if there was any uncertainty about the orbital calculations performed or if the final launch vehicle results in an orbital decay period greater than calculated.

Since the mission will utilise a LEO, it should passively deorbit over time by atmospheric drag. The orbit lifetime can be calculated once the launch epoch (solar cycle), mass, altitude, and surface area of the satellite is known. If the orbital lifetime is expected to exceed 25 years, it can be reoriented into a high-drag configuration to expedite its de-orbit.

Debris Mitigation

As access to space becomes cheaper and easier, space will become more and more crowded. Space debris is monitored by several interested parties including NASA's Orbital Debris Programme Office. As of 2015, there were no known collisions between active or inactive CubeSats and other objects in LEO, but there were more than 360,000 close calls, where CubeSats entered within 5 km of other orbital bodies[43]. The chances of collision are expected to increase, becoming a larger hazard by 2020[40]. Harris[43] shares similar findings from the Debris Analysis and Monitoring Architecture to the Geosynchronous Environment (DAMAGE) model that identifies by 2043, CubeSats will be involved in millions of close call approaches with a small amount resulting in collisions. A large amount of these close calls was found to be by CubeSats operating in SSOs.

Since the proposed mission will contribute to the ever-crowded space of LEO, the possibility of a collision has to be considered. One option that could be used as an avoidance strategy is the use of the onboard ADCS. If the satellite does not have a propulsion system to quickly raise or lower its orbit, the CubeSat should re-orientate itself into a low or high drag configuration using the ADCS (where the CubeSat is aligned with, or perpendicular to the direction of travel respectively). A CubeSat can take advantage of the atmospheric drag to decelerate and accelerate which in turn raises and lowers its orbit. While slow to change, this orbital manoeuvring may prove to be enough to avoid a collision, provided the future operations team can monitor space debris.

CONCLUSION

Earth's oceans are home to countless species of living organisms and changes must be made now to protect their habitat. As a species, we are fully aware of our excessive plastic consumption, and it has been recognised by the United Nations Foundation as one of the worlds Sustainable Development Goals to beat plastic pollution and save life below water.

The proposed mission has been identified to enhance and expand the current understanding of plastic waste in the GPGP. The mission has been developed to a point where a concept of operation has been produced detailing the proposed satellite's lifetime from launch to decommissioning and the crucial phases whereby data is collected and transmitted. The satellite mission will provide vital information needed to fully gain an understanding of the vast scale and the problem of the GPGP. The observation will cover the whole expanse of the garbage patch, plotting data points on a map to highlight areas of floating plastic debris. In time, this data can be used by targeted clean up missions, which can use the latest technological advancements to begin removing the colossal amount of waste from our oceans.

Until recently technology was not available to observe floating plastics from space, but developments in imaging capability means there are payloads that show promising indications their observation may now be possible. The next stage would be to use a Systems Engineering approach to design a CubeSat that can conduct the proposed mission.

REFERENCES

1. The Ocean Cleanup, "The Great Pacific Garbage Patch," 2020. Available from: https://theoceancleanup.com/great-pacific-garbage-patch/. [Accessed 22 May 2021].

2. Lebreton, L., Slat, B., Ferrari, F., Sainte-Rose, B., Aitken, J., Marthouse, R., Hajbane, S., Cunsolo, S., Schwarz, A., Levivier, A., Noble, K., Debeljak, P., Maral, H., Schoeneich-Argent, R., *et al*., "Evidence that the Great Pacific Garbage Patch is rapidly accumulating plastic," Scientific Reports, Vol. 8, March 2018. Available from: https://doi.org/10.1038/s41598-018-22939-w.

3. Perez, F., "Caretta Caretta Trapped". World Press Photo [online], June 2016. Available from:

https://www.worldpressphoto.org/collection/photo/2017/28790/1/2017-Francis-Perez-NA1. [Accessed 22 May 2021].

4. Chen, Q., Reisser, J., Cunsolo, S., Kwadijk, C., Kotterman, M., Proietti, M., Slat, B., Ferrari, F.F., Schwarz, A., Levivier, A., Yin, D., Hollert, H., and A.A. Koelmans, "Pollutants in Plastics within the North Pacific Subtropical Gyre," Environmental Science and Technology, vol. 52, No. 2, November 2017. Available from: https://doi.org/10.1021/acs.est.7b04682.
5. Biermann, L., Vincente, V.M., Sailley, S., Mata, A., and C. Steele, "Towards a method for detecting macroplastics by satellite: examining Sentinel-2 earth observation data for floating debris in the coastal zone," Geophysical Research Abstracts, vol. 21, April 2019. Available from: https://meetingorganizer.copernicus.org/EGU2019/EGU2019-17469.pdf.
6. Hambling, D., "How Small Satellites Will Help Police Earth's Vast Oceans," February 2019. Available from: https://www.popularmechanics.com/space/satellites/a26112020/satellites-fishing/. [Accessed 22 May 2021].
7. Kornei, K., "Satellite imagery reveals plastic garbage in the ocean," Eos, vol. 100, April 2019. Available from: https://doi.org/10.1029/2019EO121179.
8. Clark, M., "'Europe's Landsat' in the starting blocks," Spaceflight Now, June 2015. Available from: https://spaceflightnow.com/2015/06/21/europes-landsat-in-the-starting-blocks/. [Accessed 22 May 2021].
9. Micalizio, C.-S. and M. MacPhee, "Ocean Gyre," National Geographic Society, October 2014 Available from: https://www.nationalgeographic.org/encyclopedia/ocean-gyre/. [Accessed 22 May 2021].
10. Quibb, L., "Professor Quibb: Ocean Currents and the Thermohaline Circulation," February 2019. Available from: http://quibb.blogspot.com/2019/02/ocean-currents-and-thermohaline.html. [Accessed 22 May 2021].
11. Chenillat, F., Huck, T., Maes, C., Grima, N. and B. Blanke, "Fate of floating plastic debris released along the coasts in a global ocean model," Marine Pollution Bulletin, vol. 165, April 2021. Available from: https://doi.org/10.1016/j.marpolbul.2021.112116.
12. van der Mheen, M., Pattiaratchi, C., and E. van Sebille, "Role of Indian Ocean Dynamics on Accumulation of Buoyant Debris," Journal of Geophysical Research: Oceans, vol. 124, No. 4, March 2019. Available from: https://doi.org/10.1029/2018JC014806.
13. van der Mheen, M., Pattiaratchi, C. and E. van Sebille, "There's no 'garbage patch' in the Southern Indian Ocean, so where does all the rubbish go?," The Conversation, April 2019. Available from: https://theconversation.com/theres-no-garbage-patch-in-the-southern-indian-ocean-so-where-does-all-the-rubbish-go-114439?gclid=EAIaIQobChMIzP7F5KOS6AIVixnTCh1wsQcBEAMYASAAEgI-Y_D_BwE. [Accessed 22 May 2021].
14. Kane, I.A., Clare, M.A., Miramontes, E., Wogelius, R., Rothwell, J.J., Garreau, P. and F. Pohl, "Seafloor microplastic hotspots controlled by deep-sea circulation," Science, vol. 368, No. 6495, June 2020. Available from: https://science.sciencemag.org/content/368/6495/1140.
15. Stevens, A., "Plastic trash rides ocean currents to the Arctic," Science News for Students, May 2017. Available from: https://www.sciencenewsforstudents.org/article/plastic-trash-rides-ocean-currents-arctic. [Accessed 22 May 2021].
16. Silvestrova, K. and N. Stepanova, "The distribution of microplastics in the surface layer of the Atlantic Ocean from the subtropics to the equator according to visual analysis," Marine Pollution Bulletin, vol. 162, January 2021. Available from: https://doi.org/10.1016/j.marpolbul.2020.111836.
17. Welden, N.A.C., and A.L. Lusher, "Impacts of changing ocean circulation on the distribution of marine microplastic litter," Integrated Environmental Assessment and Management, vol. 13, No. 3, April 2017. Available from: http://doi.wiley.com/10.1002/ieam.1911.
18. Murray, C.C., Maximenko, N. and S. Lippiatt, "The influx of marine debris from the Great Japan Tsunami of 2011 to North American shorelines," Marine Pollution Bulletin, vol. 132, July 2018. Available from: https://doi.org/10.1016/j.marpolbul.2018.01.004.

19. Jambeck, J.R., Geyer, R., Wilcox, C., Siegler, T.R., Perryman, M., Andrady, A., Narayan, R. and K.L. Law, "Plastic waste inputs from land into the ocean," Science, vol. 347, No. 6223, February 2015. Available from: https://science.sciencemag.org/content/347/6223/768.

20. Bishop, G., Styles, D. and P.N.L. Lens, "Recycling of European plastic is a pathway for plastic debris in the ocean," Environment International, vol. 142, September 2020. Available from: https://doi.org/10.1016/j.envint.2020.105893.

21. Ritchie, H. and M. Roser, "Plastic Pollution," Our World In Data, September 2018. Available from: https://ourworldindata.org/plastic-pollution. [Accessed 22 May 2021].

22. Lebreton, L.C.M., Van Der Zwet, J., Damsteeg, J.W., Slat, B., Andrady, A. and J. Reisser, "River plastic emissions to the world's oceans," Nature Communications, vol. 8, No. 1, June 2017. Available from: https://doi.org/10.1038/ncomms15611.

23. Turner, A., Williams, T. and T. Pitchford, "Transport, weathering and pollution of plastic from container losses at sea: Observations from a spillage of inkjet cartridges in the North Atlantic Ocean," Environmental Pollution, vol. 284, September 2021. Available from: https://doi.org/10.1016/j.envpol.2021.117131.

24. World Shipping Council, "Containers Lost At Sea – 2020 Update," 2020. Available from: https://www.worldshipping.org/Containers_Lost_at_Sea_-_2020_Update_FINAL_.pdf. [Accessed 22 May 2021].

25. Galafassi, S., Nizzetto, L. and P. Volta, "Plastic sources: A survey across scientific and grey literature for their inventory and relative contribution to microplastics pollution in natural environments, with an emphasis on surface water," Science of the Total Environment, vol. 693, November 2019. Available from: https://doi.org/10.1016/j.scitotenv.2019.07.305.

26. Samuels, C., "MOL Comfort Accident: The Worst Shipping Disaster in History," Trade Risk Guaranty Blog, July 2019. Available from: https://traderiskguaranty.com/trgpeak/mol-comfort-worst-shipping-disaster/. [Accessed 22 May 2021].

27. Lebreton, L.C.M., Greer, S.D. and J.C. Borrero, "Numerical modelling of floating debris in the world's oceans," Marine Pollution Bulletin, vol. 64, No, 3, March 2012. Available from: https://www.sciencedirect.com/science/article/abs/pii/S0025326X11005674.

28. Maximenko, N., Corradi, P., Law, K.L., Van Sebille, E., Garaba, S.P., Lampitt, R.S., Galgani, F., Martinez-Vicente, V., Goddijn-Murphy, L., Veiga, J.M., Thompson, R.C., Maes, C., Moller, D., Löscher, C.R., Addamo, A.M., *et al*., "Toward the Integrated Marine Debris Observing System," Frontiers in Marine Science, August 2019. Available from: https://doi.org/10.3389/fmars.2019.00447.

29. Garaba, S.P. and H.M. Dierssen, "An airborne remote sensing case study of synthetic hydrocarbon detection using short wave infrared absorption features identified from marine-harvested macro- and microplastics," Remote Sensing of Environment, vol. 205, February 2018. Available from: https://doi.org/10.1016/j.rse.2017.11.023.

30. Zeiss, "Near Infrared Spectroscopy (NIRS)." Available from: https://www.zeiss.com/spectroscopy/solutions-applications/measuring-principle/near-infrared-spectroscopy.html#the-science. [Accessed 22 May 2021].

31. Zhu, S., Chen, H., Wang, M., Guo, X., Lei, Y. and G. Jin, "Plastic solid waste identification system based on near infrared spectroscopy in combination with support vector machine," Advanced Industrial and Engineering Polymer Research, vol. 2, No, 2 April 2019. Available from: https://doi.org/10.1016/j.aiepr.2019.04.001.

32. Petsko, E., "3 misconceptions about the Great Pacific Garbage Patch," Oceana, September 2019. Available from: https://oceana.org/blog/3-misconceptions-about-great-pacific-garbage-patch. [Accessed 22 May 2021].

33. Biermann, L., Clewley, D., Martinez-Vicente, V. and K. Topouzelis, "Finding Plastic Patches in Coastal Waters using Optical Satellite Data," Scientific Reports, vol. 10, No. 1, April 2020. Available from: https://doi.org/10.1038/s41598-020-62298-z.

34. White, S.N., Kirkwood, W., Sherman, A., Brown, M., Henthorn, R., Salamy, K., Walz, P., Peltzer, E.T. and P.G. Brewer, "Instruments and

Methods Development and deployment of a precision underwater positioning system for in situ laser Raman spectroscopy in the deep ocean," Deep Sea Research Part 1: Oceanographic Research Papers, vol. 52, No. 12 December 2005. Available from: https://doi.org/10.1016/j.dsr.2005.09.002.

35. Kraetzig, N.M., "5 Things To Know About NDVI (Normalized Difference Vegetation Index)," UP42, September 2020. Available from: https://up42.com/blog/tech/5-things-to-know-about-ndvi. [Accessed 22 May 2021].
36. GISGeography, "What is NDVI (Normalized Difference Vegetation Index)," GISGeography, December 2020. Available from: https://gisgeography.com/ndvi-normalized-difference-vegetation-index/. [Accessed 22 May 2021].
37. Earth Observing System, "NDVI", Earth Observing System. Available from: https://eos.com/make-an-analysis/ndvi/. [Accessed 22 May 2021].
38. European Space Agency, "Sentinel - Radiometric Resolutions." Available from: https://sentinel.esa.int/web/sentinel/user-guides/sentinel-2-msi/resolutions/radiometric. [Accessed 22 May 2021].
39. Chin, J., Coelho, R., Foley, F., Johnstone, A., Nugent, R., Pignatelli, D., Pignatelli, S., Powell, N., Puig-Suari, J., Atkinson, W., Dorsey, J., Higginbotham, S., Krienke, M., Nelson, K., Poffenberger, B., *et al*., "CubeSat 101: Basic Concepts and Processes for First-Time CubeSat Developers," NASA, 2017. Available from: https://www.nasa.gov/sites/default/files/atoms/files/nasa_csli_cubesat_101_508.pdf. [Accessed 22 May 2021].
40. Selding, P., "1 in 5 Cubesats Violates International Orbit Disposal Guidelines," SpaceNews, July 2015. Available from: https://spacenews.com/1-in-5-cubesats-violate-international-orbit-disposal-guidelines/. [Accessed 22 May 2021].
41. Lewis, H., "Alignment of Capability and Capacity for the Objective of Reducing Debris," Cordis – Research EU, vol. 32, February 2014. Available from: https://cordis.europa.eu/project/id/262824/reporting.
42. Committee on the Peaceful Uses of Outer Space, "Compendium of space debris mitigation standards adopted by States and international organizations," COPUOS 57th session, June 2014. Available from: https://www.unoosa.org/pdf/limited/l/AC105_2014_CRP13E.pdf. [Accessed 22 May 2021].
43. Harris, G., "Space debris expert warns of increasing CubeSat collision risk," Phys.org, September 2014. Available from: https://phys.org/news/2014-09-space-debris-expert-cubesat-collision.html. [Accessed 22 May 2021].